Collapse and Swelling of Thermally Sensitive Poly(*N*-isopropylacrylamide) Brushes Monitored with a Quartz Crystal Microbalance

Guangming Liu and Guangzhao Zhang*

Hefei National Laboratory for Physical Sciences at Microscale, Department of Chemical Physics, University of Science and Technology of China, Hefei, Anhui, China

Received: July 13, 2004; In Final Form: October 15, 2004

Thermally sensitive poly(*N*-isopropylacrylamide) (PNIPAM) brushes grafted on SiO_2-coated quartz crystal surface were prepared with a surface-immobilized initiator. Using quartz crystal microbalance (QCM), we investigated the collapse and swelling of the brushes in water in real time. Both frequency and dissipation of PNIPAM brushes were found to gradually change throughout a temperature range 20−38 °C, indicating that PNIPAM brushes undergo a continuous collapse transition in contrast with PNIPAM chains free in dilute solution exhibiting a sharp coil-to-globule transition. This result is in accordance with the previous theoretical prediction. The nonuniformity and stretching of PNIPAM brushes as well as the cooperativity between collapse and dehydration transitions are thought to be responsible for the continuity. On the other hand, a hysteresis was also observed in the cooling process. This is not only due to the intrachain and interchain interactions formed in the collapsed state but also to the nonuniform structure and stretching of the high-density brushes.

Introduction

Polymer chains grafted at one or both ends onto a surface form a polymer brush when the grafting density is so high that the chains have to stretch outward from the surface without any overlapping in good solvent due to the effect of exclusion.[1−3] Such a coil-to-brush transition has attracted much interest with various implications,[4−20] such as in colloidal stabilization,[16] self-assembly of polymer chains,[17] and tribology.[18] It has been theoretically predicted that each stretched chain in a polymer brush will gradually shrink and finally collapse into a globule as the solvent quality decreases due to the constraint of the chains on surface, in contrast with a linear chain free in solution exhibiting a discontinuous coil-to-globule transition.[4−6] Although some of the experimental results support such a prediction,[21−27] because systematically experimental investigations are very limited,[21] the conformation change of densely grafted linear polymer chains with a decreasing solvent quality still remains an open question. One of the difficulties or experimental challenges is how to anchor the chains on a surface with a high grafting density.

It is well-known that PNIPAM exhibits a lower critical solution temperature (LCST) at ∼32 °C in water;[28−30] namely, a PNIPAM chain swells with a random coil conformation at lower temperatures but collapses into a globule at a temperature above the LCST. PNIPAM brushes in water have been investigated by conveniently adjusting the solvent quality via temperature.[21,22,31−34] Contact angle measurements[32,33] indicated that a PNIPAM brush showed a sharp solubility transition near the LCST, similar to what happened to PNIPAM chains free in water. On the other hand, using surface plasmon resonance (SPR), Balamurugan et al.[21] recently showed that the collapse of the chains in a PNIPAM brush was indeed gradual.

The quartz crystal microbalance (QCM) has been widely used to determine properties of the thin film in vacuum or air based on Sauerbrey equation.[35,36] Recently, its applications extended to the study on adsorption, conformation, and interactions of macromolecules in solution.[27,37−43] Particularly, Domack et al.[27] investigated the swelling of polystyrene brushes in cyclohexane and found the brushes exhibit a continuous transition. In the present work, we directly grew PNIPAM brushes with high density on the surface of QCM sensor and studied their collapse and swelling in water.

Experimental Section

Materials. Isopropylacrylamide from Aldrich was recrystallized three times in a benzene/*n*-hexane mixture. *N*,*N*-Dimethylformamide (DMF) was dried with anhydrous $CaSO_4$ and distilled under a vacuum before use. 4,4′-Azobis(4-cyanovaleric acid) (ABCA), 3-(aminopropyl)trimethoxysilane (APTMS), 1,3-dicyclohexylcarbodiimide (DCC) were from Acros and used as received. The SiO_2-coated crystal surface was cleaned using Piranha solution composed of one part H_2O_2 and three parts H_2SO_4, then rinsed with Milli-Q water, and blown dry with a stream of nitrogen gas. [***Caution***: Piranha is an aggressive and explosive chemical. Never mix piranha waste with solvents. Check the safety precautions before using it.] Several wash/dry cycles were performed until concordant frequencies were obtained. Scheme 1 describes the graft polymerization of NIPAM onto a crystal surface. APTMS was used to immobilize the initiator on the crystal surface because the Si−O bond formed by APTMS and SiO_2 surface with a bond energy of 452kJ/mol[44] is very stable even at a high temperature. The APTMS monolayer was formed by immersing the crystal in a 1 mM APTMS solution in ethanol for 40 min. The surfaces were then washed with ethanol and water, blown with nitrogen gas, and baked at 120 °C in an oven for 30 min to complete the formation of Si−O bond.[45] The APTMS modified surface was then exposed to 40 mL solution in DMF containing 0.2 g of ABCA, 2 g of DCC, and 50 μL of pyridine as the catalyst, so that the initiator (ABCA) was rooted on the SiO_2 surface. The reaction was carried at room temperature for 8 h. Then, the crystal was immersed in an aqueous solution of 0.5 g of NIPAM with one side covered with a protective casing made of Teflon. The graft polymerization was conducted at 60 °C for 8 h under a nitrogen blanket. The quartz crystal grafted with PNIPAM was rinsed with Milli-Q water until stable frequencies were

10.1021/jp046903m CCC: $30.25
Published on Web 12/01/2004

SCHEME 1

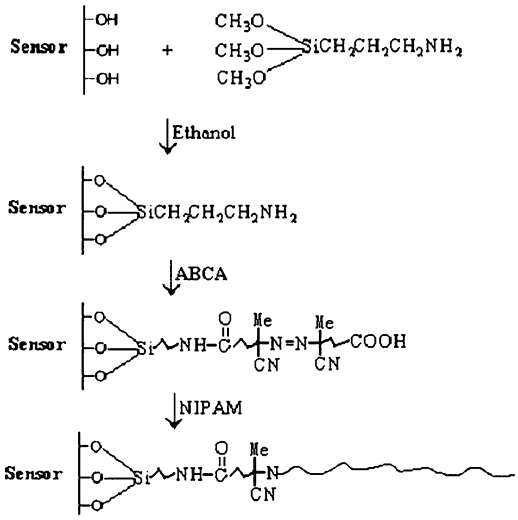

obtained so that the PNIPAM chains physically absorbed on the grafting layer were completely removed. Then, it was blown dry with nitrogen, and further dried in a vacuum oven at room temperature for 24 h.

The apparent molecular mass of PNIPAM chains grafted on SiO_2 surface was determined to be $M_w = 9.3 \times 10^5$ g/mol by static laser light scattering for the nonattached PNIPAM chains free in solution during polymerization. The polydispersity of PNIPAM was evaluated to be $M_w/M_n \approx 2$ by dynamic laser light scattering.[46] Assuming that PNIPAM layer is rigid and evenly distributed on the surface of QCM sensor, the thickness (H_{dry}) of the dry tethered PNIPAM chains was evaluated to be ~41 nm by QCM as discussed below. From the molecular weight and the mass per area, the distance between two anchoring sites was evaluated to be $d \sim 4$ nm. Because $H_{dry} \gg d$, the tethered PNIPAM chains form brushes. The crystal grafted with PNIPAM brushes had been immersed in water at 20 °C for at least 1 week before the QCM measurements so that the brushes were sufficiently swollen.

QCM-D Technique. Quartz crystal microbalance with dissipation monitoring (QCM-D) having an AT-cut quartz crystal with a fundamental resonant frequency of 5 MHz and a diameter of 14 mm was from Q-sense AB.[47] The quartz crystal with a 50 nm thick SiO_2 layer on the top of the gold electrode was mounted in a fluid cell with one side exposed to the solution in the experiments. The effect of surface roughness[48] is neglected because the root-mean-square (rms) is less than 3 nm. The constant (C) of the crystal used here is 17.7 ng/(cm^2 Hz), the frequency shift is measurable to within ±1 Hz in aqueous medium, and the temperature was controlled in the range ±0.02 °C.

When the quartz crystal is excited to oscillation in the thickness shear mode at its fundamental resonant frequency f_0 by applying a RF voltage across the electrodes near the resonant frequency, a small layer added to the electrodes induces a decrease in resonant frequency. If the layer is evenly distributed and much thinner than the mass of the crystal, the frequency shift (Δf) can be related to the layer mass (Δm) by the Sauerbrey equation.[35]

$$\Delta m = -\frac{\rho l}{f_0}\frac{\Delta f}{n} \quad (1)$$

where ρ and l are the specific density and thickness of the quartz crystal, respectively, and $n = 1, 3, 5, \ldots$. The dissipation factor is defined by $\Delta D = E_{dissipated}/2\pi E_{stored}$, where $E_{dissipated}$ and E_{stored} are the dissipated energy and stored energy during one oscillation.[47] The measurement of energy dissipation (ΔD) is based on the fact that the voltage over the crystal decays exponentially as a damped sinusoidal when the driving power to a piezoelectric oscillator is switched *off*. By switching the driving voltage on and off periodically, the series resonant frequency and the dissipation factors are obtained simultaneously. Δf and ΔD values from the fundamental were usually noisy because of insufficient energy trapping and therefore discarded.[49]

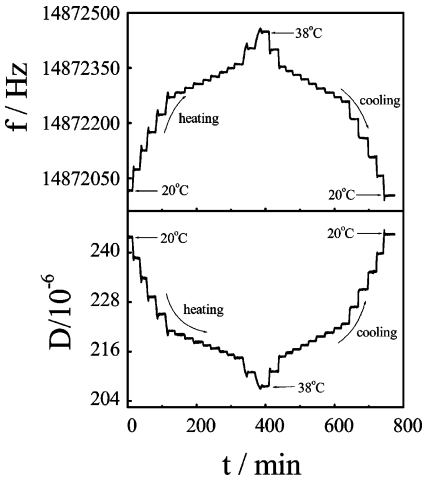

Figure 1. Time dependence of frequency (f) and dissipation factor (D) of SiO_2-coated quartz crystal grafted with PNIPAM brushes at $n = 3$.

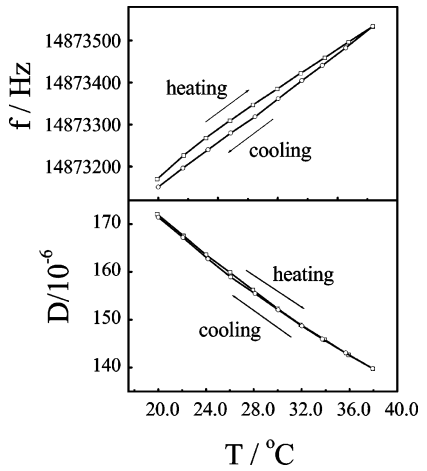

Figure 2. Temperature dependence of frequency (f) and dissipation factor (D) of a bare SiO_2-coated quartz crystal at $n = 3$.

Results and Discussion

Figure 1 shows temperature effects on frequency (f) and dissipation (D) of quartz resonator grafted with PNIPAM brushes in real time, where frequency attained a constant value at each temperature; i.e., the fluctuation of frequency was within ±2 Hz in half an hour. It can be seen that in either the heating or cooling process, the frequency increases with temperature increasing, whereas the dissipation decreases. However, the changes of frequency and dissipation not only come from PNIPAM brushes but also from the crystal resonator itself and the water surrounding them.

Figure 2 shows when the bare SiO_2-coated crystal resonator without PNIPAM brushes is immersed in water, the frequency also increases with temperature increasing, while the dissipation factor decreases. It is known that the frequency response of a

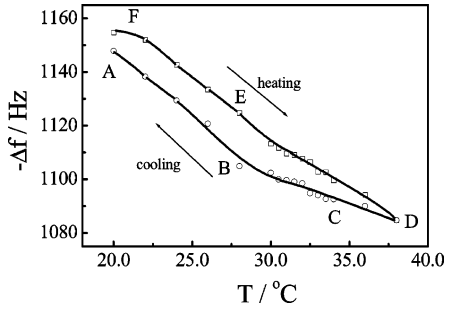

Figure 3. Temperature dependence of frequency shift ($-\Delta f$) of PNIPAM brushes at $n = 3$.

quartz resonator immersed in a Newtonian liquid can be quantitatively described by the relation derived by Kanazawa and Gordon,[50]

$$\Delta f = -n^{0.5} f_0^{1.5} (\eta\rho/\pi\mu_q\rho_q)^{0.5} \quad (2)$$

where f_0 is the fundamental frequency, n is the harmonic number, ρ_q and μ_q are the density and shear modulus of quartz, and ρ and η are the density and viscosity of the liquid medium, respectively. The dissipation response is given by[51]

$$\Delta D = 2(f_0/n)^{0.5} (\eta\rho/\pi\mu_q\rho_q)^{0.5} \quad (3)$$

Equations 2 and 3 indicate that the changes of frequency and dissipation of the bare crystal resonator can be attributed to the change in viscosity and density of water or their product as a function of temperature. On the other hand, a combination of eqs 2 and 3 yields

$$\frac{\Delta D}{\Delta f} = \frac{-2}{n f_0} \quad (4)$$

Then, $-\Delta D/\Delta f = 1.33 \times 10^{-7}$ when $n = 3$ and $f_0 = 5$ MHz. $-\Delta D/\Delta f$ values from Figure 2 are apparently smaller than 1.33×10^{-7}. The inconsistency is easily explained by temperature−frequency coupling because the frequency of a quartz crystal responds to temperature depending on the crystal cut, whereas the dissipation does not. On the other hand, there exists a hysteresis for the frequency change in the heating and cooling cycle. A similar behavior was also observed in a recent investigation.[39] Therefore, the temperature effects on bare crystal resonator in water must be taken into account. Here, the frequency shift (Δf) and dissipation shift (ΔD) of PNIPAM brushes were evaluated by subtracting the values for the bare crystal resonator from the corresponding values measured for the crystal grafted with PNIPAM brushes.

Figure 3 shows the temperature dependence of frequency shift ($-\Delta f$) of PNIPAM brushes in one heating-and-cooling cycle. It can be seen that $-\Delta f$ gradually decreases with the temperature increasing in the heating process over the range 20−38 °C. At low temperature, water is a good solvent for PNIPAM, PNIPAM chains strongly interact with water molecules. As temperature increases, dehydration occurs and PNIPAM chains gradually collapse, leading to the decrease of $-\Delta f$. On the other hand, a collapsed PNIPAM brush became swollen with temperature decreasing in the cooling process reflecting in the increase of $-\Delta f$. The continuous changes of frequency in both heating and cooling process are markedly different from the sharp coil-to-globule transition of individual PNIPAM chains free in water.[52] We will come back to this point later.

It should be noted that a frequency shift of a viscoelastic polymer layer on a quartz crystal is generally influenced by its

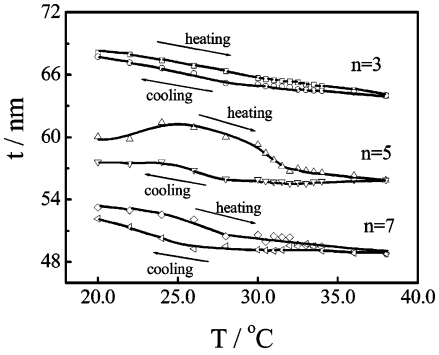

Figure 4. Temperature dependence of apparent thickness (t) of PNIPAM brushes at different harmonics.

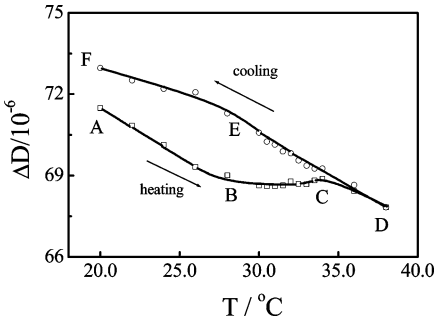

Figure 5. Temperature dependence of dissipation shift (ΔD) of PNIPAM brushes at $n = 3$.

thickness, density, storage, and loss moduli.[53] So far, it is difficult to experimentally separate their contributions to frequency response. Mathematical fitting with approximations and assumptions or other in situ techniques has to be used.[54] Δf and ΔD data collected at multiple harmonics are helpful for us to determine the viscoelastic properties of the brushes. The layer studied here is much thinner than the quartz crystal,[47] the thickness and the loss modulus due to hydration or dehydration should have dominant effects on the frequency shift and dissipation. Accordingly, the apparent thickness can be estimated using Sauerbrey equation (eq 5). This can at least give a qualitatively correct picture of hydrodynamic behavior of PNIPAM brushes.

$$t = \frac{\Delta m}{\rho} = \frac{-C\Delta f}{n\rho} \quad (5)$$

where $\rho \sim 1000$ kg/m^3 is used as the average density of PNIPAM and water.

Figure 4 shows the temperature dependence of apparent thickness (t) of PNIPAM brushes at different harmonics. The frequency dependence of the apparent thickness indicates that the brushes are viscoelastic. Figure 4 also shows the thickness of PNIPAM brushes for the third overtone at swollen and collapsed states are 68 and 64 nm, respectively, implying that only partial hydration and dehydration of the brushes happen because of their high density. In other words, the stretching of PNIPAM chains restrains their hydration at low temperature and dehydration at a temperature higher than 32 °C.

Figure 5 shows the temperature dependence of the dissipation change (ΔD) in one heating and cooling cycle. Dissipation of a viscoelastic polymer layer on quartz resonator is heavily influenced by its structure. A dense or rigid layer has a small dissipation of energy, whereas the dissipation of a looser or more flexible structure is larger.[47] The dissipation in Figure 5 decreases with temperature increasing in the heating process, indicating that PNIPAM brushes gradually collapse into a more

compact structure. Nevertheless, there is an observed transition ~34 °C. In the cooling process, the dissipation smoothly increases with temperature decreasing over a range of temperature from 38 to 20 °C, indicating that the collapsed brushes become more swollen and flexible. Unlike the case in the heating process, no observed transitions occur in the cooling process. On the other hand, Figure 5 also shows that a ΔD value in the cooling process is generally larger than that in the heating process at the same temperature, whereas an opposite trend is found for Δf data shown in Figure 3. The phenomenon arises from the tails on the outer layer of the brushes, which have critical effects on the dissipation. In the heating process, PNIPAM chains collapsing from the stretching state do not have a chance to produce flexible and random tails. In the cooling process, the brushes begin to swell from their outer layer to inner core, resulting in some swollen tails that behave like short chains tethered on the inner layer. At the initial stage, because the distance between two ends of the tails is large, no stretching occurs, and the random and flexible tails give rise to a marked increase of ΔD further smoothing the transition. Because the amount of water molecules coupling to the tails is still limited, $-\Delta f$ only increases a little. Further cooling leads the segments of PNIPAM closer to the sensor surface to be swollen. The tails would stretch with the distance between their ends increasing. However, we found that it took about 1 week for PNIPAM brushes to complete the swelling at 20 °C. In the time we observed, the flexible and random tails did not completely stretch yet, which is evidenced by the facts that both ΔD and Δf were not back to their original values at 20 °C, shown in Figures 3 and 5. The slow rehydration further indicates that the transition only appears to be continuous because the kinetics is much slower than the time scale of the experiment.

The continuous transition shown in Figures 3 and 5 was theoretically predicted by mean-field calculations[5] and simulations,[6] and also experimentally observed for polystyrene brushes[27] in cyclohexane and PNIPAM brushes in water.[21] Such a continuous transition was thought to arise from the high density and nonuniformity of the chains, which lead to a spectrum of the collapse rates.[1−3] The surface constraint enhancing the interchain interactions can also broaden the transition.[5] It should be noted that the collapse of a polymer brush was theoretically predicted to be accompanied by a solubility transition,[5,7] the cooperativity of the two transitions should also influence the continuity. Actually, it is found that cooperativity plays an essential role in continuous volume change of some hydrogels[55] and DNA condensation.[56] So far, the effect of cooperativity has not been recognized for collapse of a polymer brush. This is probably because the collapse and solubility transitions are difficult to probe separately. In the present study, Δf is mainly caused by the hydration and dehydration, whereas ΔD is due to the conformational change. The relation between ΔD and Δf is expected to provide useful information about the cooperativity and the kinetic process of the collapse transition.

Figure 6 clearly reveals that there exist three kinetic processes in the heating process. When $T < 28$ °C (A to B), ΔD decreases with $-\Delta f$ decreasing, implying that the shrinking and dehydration of PNIPAM chains happen simultaneously. In the range 28 °C $< T <$ 34 °C (B to C), ΔD slightly changes as $-\Delta f$ decreases. As in the case of individual PNIPAM chains,[52] PNIPAM brushes are partially collapsed in this range of temperature. The conformational change of the collapsed brushes is very limited so that ΔD slightly changes. On the other hand, not all the detached water molecules during shrinking at $T <$ 28 °C can leave PNIPAM brushes immediately, some of them

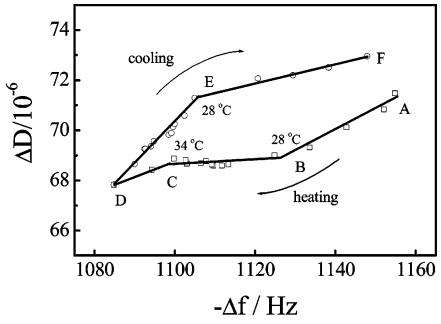

Figure 6. Frequency shift ($-\Delta f$) dependence of dissipation shift (ΔD) of PNIPAM brushes at $n = 3$.

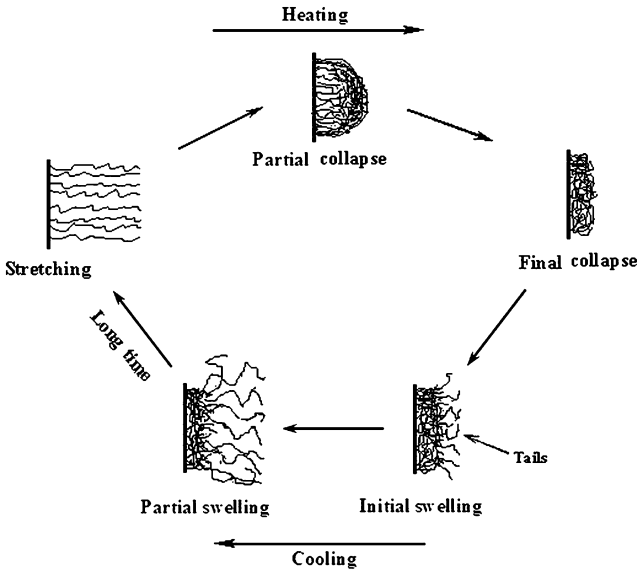

Figure 7. Schematic illustration of collapse and swelling of PNIPAM brushes.

are trapped in the dense brushes. As temperature increases, the trapped water molecules gradually diffuse out of the brushes, leading to a frequency change. Obviously, the cooperativity between the collapse and dehydration is weak due to the retarded dehydration, which is also responsible for the continuous collapse transition. Further heating overcoming the energy barrier for the stretching leads to more collapse and dehydration reflected in the decreases of ΔD and $-\Delta f$ at $T >$ 34 °C (C to D). In the cooling process, when the temperature is higher than 28 °C (D to E), ΔD rapidly increases with $-\Delta f$ increasing, suggesting that the tails on outer layer are hydrated and flexible. When $T <$ 28 °C (E to F), ΔD slows down its increase because the solvated chains in the outer layer tend to stretch and pack more densely. Note that for the same $-\Delta f$, a ΔD value in the cooling process is always higher than that in the heating process, further indicating that the flexible tails have a pronounced effect on the dissipation.

Figures 3, 5, and 6 also show a hysteresis in the heating and cooling cycle, indicating an irreversible collapse transition. This behavior was also observed for PNIPAM chains free in dilute solution,[52] which was attributed to the intrachain interactions formed in the collapsed state. Such interactions hinder the hydration of the collapsed chains in the cooling process. For PNIPAM brushes, besides the knotting and entangling of PNIPAM chains due to the intrachain and interchain interactions in the collapsed state, the nonuniformity and the stretching of the brushes are thought to further enlarge the hysteresis. Summarizing the above discussion, Figure 7 schematically illustrates the collapse and swelling of PNIPAM brushes.

Conclusion

We have investigated the temperature dependence of collapse and swelling of PNIPAM brushes grafted on SiO_2 surface in water with a quartz crystal microbalance. PNIPAM brushes were found to exhibit a continuous collapse over a temperature range of 20−38 °C, reflecting the gradual changes in frequency and dissipation. In addition to nonuniformity and stretching of the brushes, the cooperativity between collapse and dehydration transitions is thought to be responsible for such a continuous collapse. Our results support the theoretical prediction developed by Zhulina et al.[5] The results also reveal that there exists a hysteresis in the swelling of the collapsed chains, which is attributed to the intrachain and interchain interactions formed in the collapsed state at higher temperatures and the nonuniformity of the brushes.

Acknowledgment. The financial support of the National Major Research Plan Projects (90303021) and CAS "Bai Ren" Project is gratefully acknowledged.

References and Notes

(1) Alexander, S. *J. Phys. (Paris)* **1977**, *38*, 983.
(2) de Gennes, P. G. *Macromolecules* **1980**, *13*, 1069.
(3) Halperin, A.; Tirrell, M.; Lodge, T. P. *Adv. Polym. Sci.* **1991**, *100*, 31.
(4) Milner, S. T. *Science* **1991**, *251*, 905.
(5) Zhulina, E. B.; Borisov, O. V.; Pryamitsyn, V. A.; Birshtein, T. M. *Macromolecules* **1991**, *24*, 140.
(6) Grest, G. S.; Murat, M. In *Monte Carlo and Molecular Dynamics Simulations in Polymer Science*; Binder K., Ed.; Clarendon: Oxford, U.K., 1994.
(7) Szleifer, I.; Cargnano, M. A. *Adv. Chem. Phys.* **1996**, *94*, 165.
(8) Stuart, M. A. C.; Waajen, F. H. W. H.; Cosgrove, T.; Vincent, B.; Crowley, T. L. *Macromolecules* **1984**, *17*, 1825.
(9) Hadziioannou, G.; Patel, S.; Granick, S.; Tirrell, M. *J. Am. Chem. Soc.* **1986**, *108*, 2869.
(10) Fleer, G. J.; Stuart, M. A. C.; Scheutjens, J. M. H. M.; Cosgrove, T.; Vincent, B. *Polymers at Interfaces*, 1st ed.; Cambridge University Press: Cambridge, England, 1993.
(11) Chevalier, Y.; Brunel, S.; Le Perchec, P.; Mosquet, M.; Guicquero, J. P. *Prog. Colloid Polym. Sci.* **1997**, *105*, 66.
(12) Rustemeirer, O.; Killmann, E. *J. Colloid. Interface Sci.* **1997**, *190*, 360.
(13) Ortega-Vinuesa, J. L.; Maratin-Rodrigues, A.; Hidalgo-Alvarez, R. *J. Colloid Interface Sci.* **1996**, *184*, 259.
(14) Walker, H. W.; Grant, S. B. *J. Colloid Interface Sci.* **1996**, *179*, 552.
(15) Zhao, B.; Brittain, W. J. *Prog. Polym. Sci.* **2000**, *25*, 677.
(16) Napper, D. H. *Steric Stabilization of Colloidal Dispersions*; Academic Press: New York, 1983.
(17) Amiji, M.; Park, K. *J. Biomater. Sci. Polym. Ed.* **1993**, *4*, 217. Gast, A. P. *Langmuir* **1996**, *12*, 4060.
(18) Klein, J.; Kumacheva, E. *Science* **1995**, *269*, 816.
(19) Klein, J. *Annu. Rev. Mater Sci.* **1996**, 26, 581.
(20) van Zanten, J. H. *Macromolecules* **1994**, *27*, 6797.
(21) Balamurugan, S.; Mendez, S.; Balamurugan, S. S.; O'Brien, M. J., II; Lopez, G. Z. *Langmuir* **2003**, *19*, 2545.
(22) Zhu, P. W.; Napper, D. H. *J. Colloid Interface Sci.* **1994**, *164*, 489.
(23) Karim, A.; Satija, S. K.; Douglas, J. F.; Ankner, J. F.; Fetters, L. J. *Phys. Rev. Lett.* **1994**, *73*, 3407.
(24) Webber, R. M.; van der Linden, C. C.; Anderson, J. L. *Langmuir* **1996**, *12*, 1040.
(25) Habicht, J.; Schmidt, M.; Ruhe, J.; Johannsmann, D. *Langmuir* **1999**, *15*, 2460.
(26) Auroy, P.; Auvary, L. *Macromolecules* **1992**, *25*, 4143.
(27) Domack, A.; Prucker, S.; Rühe, J.; Johannsmann, D. *Phys. Rev. E* **1997**, *56*, 680.
(28) Heskins, M.; Guillet, J. E.; James, E. *J. Macromol. Sci., Chem.* **1968**, *A2*, 1441.
(29) Hoffman, A. S. *MRS Bull.* **1991**, *16*, 42.
(30) Schild, H. G. *Prog. Polym. Sci.* **1992**, *17*, 163 and references therein.
(31) Hu, T. J.; Wu, C. *Phys. Rev. Lett.* **1999**, *83*, 4105.
(32) Takei, Y. G.; Aoki, T.; Sanui, K.; Ogata, N.; Sakurai, Y.; Okano, T. *Macromolecules* **1994**, *27*, 6163.
(33) Zhang, J.; Pelton, R.; Deng, Y. *Langmuir* **1995**, *11*, 2301.
(34) Kidoaki, S.; Ohya, S.; Nakayama, Y.; Matsuda, T. *Langmuir* **2001**, *17*, 2402.
(35) Sauerbrey, G. *Z. Phys.* **1959**, *155*, 206.
(36) Pulker, H. K.; Decoserd, J. P., In *Applications of Piezoelectric Quartz Crystal Microbalance*, edited by Lu, C., Czanderna, A. W., Elsevier: Amsterdam, 1984.
(37) Munro, J. C.; Frank, C. W. *Macromolecules* **2004**, *37*, 925.
(38) Fu, T. Z.; Stimming, U.; Durning, C. J. *Macromolecules* **1993**, *26*, 3271.
(39) Plunkett, M. A.; Wang, Z. H.; Rutland, M. W.; Johannsmann, D. *Langmuir* **2003**, *19*, 6837.
(40) Xu, H.; Schlenoff, J. B. *Langmuir* **1994**, *10*, 241.
(41) Ivanchenko, M. I.; Kobayashi, H.; Eduard, A. K.; Dobrova, N. B. *Anal. Chim. Acta* **1995**, *314*, 23.
(42) Caruso, F.; Furlong, D. N.; Kingshott, P. *J. Colloid Interface Sci.* **1997**, *186*, 129.
(43) Hook, F.; Rodahl, M.; Brezinski, P.; Kasemo, B.; Brezinski, P. *Proc. Natl. Acad. Sci. U.S.A* **1998**, *95* (2), 12271 and references therein. Hook, F.; Kasemo, B.; Nylander, T.; Fant, C.; Scott, K.; Elwing, H. *Anal. Chem.* **2001**, *73*, 5796.
(44) Cottrell, T. L. *The Strength of Chemical Bonds*, 2nd ed; Butterworth Scientific Publications: London 1958.
(45) Sato, T.; Brown, D.; Johnson, B. F. G. *Chem. Commun*. **1997**, *11*, 1007.
(46) Chu, B.; Wang, Z.; Yu, J. *Macromolecules* **1991**, *24*, 6832.
(47) Rodahl, M.; Höök, F.; Krozer, A.; Kasemo, B.; Breszinsky, P. *Rev. Sci. Instrum.* **1995**, *66*, 3924. Voinova, M. V.; Rodahl, M.; Jonson, M.; Kasemo, B. *Phys. Scrip.* **1999**, *59*, 391.
(48) Daikhin, L.; Urbakh, M. *Faraday Discuss.* **1997**, *107*, 27. Daikhin, L.; Gileadi, E.; Katz, G.; Tsionsky, V.; Urbakh, M.; Zagidulin, D. *Anal. Chem.* **2002**, *74*, 554.
(49) Bottom, V. E. *Introduction to Quartz Crystal Unit Design*; Van Nostrand Reinhold Co.: New York, 1982.
(50) Kanazawa, K. Z.; Gordon, J. G., III. *Anal. Chem.* **1985**, *57*, 1770.
(51) Stockbridge, C. D. In *Vacuum Microbalance Techniques*; Katz, M. J., Eds.; Plenum Press: New York, 1966. Rodahl, M.; Kasemo, B. *Sens. Actuators A* **1996**, *54*, 448.
(52) Wu, C.; Zhou, S. *Macromolecules* **1995**, *28*, 5388; *Phys. Rev. Lett.* **1996**, *77*, 3053; Wu, C.; Wang, X. H. *Phys. Rev. Lett.* **1998**, *80*, 4092.
(53) Lucklum, R.; Hauptmann, P. *Meas. Sci. Technol.* **2003**, *14*, 1854 and references therein.
(54) Hillman, R. A.; Jackson, A.; Martin, S. J. *Anal. Chem.* **2001**, *73*, 540.
(55) Yoshida, R.; Uchida, K.; Kaneko, Y.; Sakai, K.; Kikuchi, A.; Sakurai, Y.; Okano, T. *Nature* **1995,** *374*, 240. Annaka, M.; Motokawa, K.; Sasaki, S.; Nakahira, T.; Kawasaki, H.; Maeda, H.; Amo, Y.; Tominaga, Y. *J. Chem. Phys.* **2000**, *113*, 5980.
(56) Iwataki, T.; Yoshikawa, K.; Kidoaki, S.; Umeno, D.; Kiji, M.; Maeda, M. *J. Am. Chem. Soc.* **2000**, *122*, 9891 and the references therein.